

Study on Mesoporous Al-SBA-15 with Enhanced Acidity and Hydrothermal Stability for Heavy Oil Hydrocracking Conversion

Lianhui Ding*, Hanaa Habboubi, Essam Sayed, Sitepu Husinsyah, Hameed Badairy, Rasha Alghamdi

Research and Development Center, Saudi Aramco, Dhahran, Saudi Arabia

Email address:

Lianhui.ding@aramco.com (L. Ding)

*Corresponding author

To cite this article:

Lianhui Ding, Hanaa Habboubi, Essam Sayed, Sitepu Husinsyah, Hameed Badairy, Rasha Alghamdi. Study on Mesoporous Al-SBA-15 with Enhanced Acidity and Hydrothermal Stability for Heavy Oil Hydrocracking Conversion. *American Journal of Materials Synthesis and Processing*. Vol. 3, No. 3, 2018, pp. 39-46. doi: 10.11648/j.ajmsp.20180303.11

Received: August 9, 2018; **Accepted:** August 20, 2018; **Published:** September 28, 2018

Abstract: To increase heavy oil conversion by hydrocracking, the larger pore opening mesoporous materials with enhanced acidity and hydrothermal stability are required. A series of mesoporous Al-SBA-15 was studied in acid-free and different HCl concentration solutions with various initial SiO₂/Al₂O₃ molar ratio. The final product samples were characterized with N₂ adsorption, SAXS/XRD, NH₃-TPD, TEM, ²⁸Si NMR, and ²⁷Al NMR. The results concluded that the acid-free and weak acidic medium favor the formation of the Al-SBA-15 with better textural properties, higher acidity, and higher wall-thickness. A considerable amount of Al was present in the tetrahedral form.

Keywords: Mesoporous Materials, SBA-15, Synthesis, Hydrocracking

1. Introduction

Hydrocracking process is one of the most important processes in modern refineries, due to its high versatility in processing different feedstocks, good product quality, and high liquid yields, especially at times when crude oil properties are getting deteriorated yearly and more environmentally friendly products are demanded. Hydrocracking catalysts play a crucial role in the process, because the catalysts determinate product selectivity, hydrogen consumption, run length, and economics.

Hydrocracking catalysts are bi-functional: cracking function contributed by the acidic sites such as amorphous oxides (silica-alumina) and/or zeolites, and hydrogenation function by the metals such as Co-Mo, Ni-Mo, or Ni-W. Before 1960, the amorphous silica alumina catalysts were widely used. After that, via intense researches and studies, the zeolites (mainly zeolite Y and beta) were found to have much higher acidity, higher thermal/hydrothermal stability, and showed significant improvements in activity, ammonia tolerance, and higher gasoline selectivity. Until now, zeolite Y

or zeolite beta is still widely used cracking component for the commercialized catalysts.

Zeolite Y and beta with a 12-membered ring have maximum pore opening 7-8Å which is smaller than the sizes of the most molecules in heavy oils. To improve the large molecule diffusion inside the zeolites, great efforts were made to develop the mesoporous materials [1-4] that can be applied in heavy oil hydroprocessing. Although the mesoporous materials such as widely studied SBA-15 and M41S family have high surface area, large pore volume, and uniform hexagonal array of cylindrical mesopores [5], their lower acidity and worse thermal and hydrothermal stability compared with zeolites become big challenges in hydroprocessing application [6].

Among all the mesoporous materials studied (such as MCM-41, MCM-48, MCM-50 and SBA-15 etc.), SBA-15 has the thickest wall, and thus has higher thermal and hydrothermal stability than other mesoporous materials [7]. However, the stability is not higher enough to be used in the hydrocracking catalysts. Meanwhile, its acidity is similar to that of amorphous silica-alumina, and too low to hydroprocess

most of heavy oils. In the early stage, only pure silicon SBA-15 was synthesized and studied in the strong acid medium. The highly acidic synthesis medium hindered the direct incorporation of metal ions, such as trivalent aluminum, into the silica framework. In order to increase the acidity of the materials, many modifications were made, such as aluminum being introduced into pure silica SBA-15, or post treatment of SBA-15 [8-13]. W. Hua and his co-workers reported an acidity enhancement method by $\text{SO}_4^{2-}/\text{ZrO}_2$ modification. Zirconium nitrate was impregnated onto SBA-15, after drying and precalcination, the precalcinated samples were treated with 0.5M of H_2SO_4 . Although the acidity was enhanced, the surface areas and pore volumes were greatly reduced from $683\text{m}^2/\text{g}$ to $<500\text{m}^2/\text{g}$ and $0.98\text{ml}/\text{g}$ to $<0.70\text{ml}/\text{g}$ respectively. C. Han *et al.* treated SBA-15 with diluted solution of aluminosilicate sol-gel, which caused a huge loss in pore volumes and surface areas (reduce half). Campos and his co-workers impregnated SBA-15 with TPABr and NH_4F to transform the amorphous wall of the mesoporous SBA-15. In acid media, the SBA-15 synthesized contained only traces of aluminum, despite the fairly high aluminum content in the original gel. Meantime, surface areas were reduced from $699\text{m}^2/\text{g}$ to $<380\text{m}^2/\text{g}$. Other methods included post synthesis alumination of mesoporous silica SBA-15 using ammonium hexafluoroaluminate, coating of alumina on the wall of SBA-15 by ammonia/water vapor induced internal hydrolysis, impregnating SBA-15 with aluminum nitrate, and then by vapor hydrolysis, and multiple grafting of Al isopropoxide in organic solvent on SBA-15. With all these methods, the aluminum species were coated on the wall of the meso SBA-15. They could only enhance the acidity to a limited extent, but led to huge loss in pore volumes and surface areas.

To simultaneously improve the acidity and stability, the best and efficient approach is to convert the amorphous silica-alumina wall to crystallized silica-alumina (zeolite type) during the synthesis, at least incorporate as large amounts of Al atoms as possible in a tetrahedral environment. Many attempts were made to achieve the goal. Wang and his co-workers reported a highly ordered SBA-15 with thick pore wall and high hydrothermal stability, which was synthesized by adding PVA powder [14]. Studies showed that direct synthesis under acid-free or very mild acid conditions significantly enhanced the acidity and hydrothermal stability of the mesoporous materials, and thus more ordered wall structure may be formed [15-17]. Because different researches used various chemicals and synthesis conditions, it is hard to compare the effect of the initial acid concentration and silica-to-alumina ratio on the main properties of the synthesis Al-SBA-15. Therefore, in this communication, under the same starting silicon and aluminum sources, the effect of initial acid concentration and silica/alumina ratio was investigated.

2. Experimental

2.1. Synthesis of Al-SBA-15

The mesoporous materials were prepared in different HCl

concentrations (0-5.0M) by using different concentrations of $\text{SiO}_2/\text{Al}_2\text{O}_3$ molar ratio (5, 20, and 50). Nonionic triblock copolymer, Pluronic P123 (Aldrich), was used as the structure-directing agent (SDA). Tetraethyl orthosilicate (TEOS, Fluka) and aluminum sulfate 18-hydrate ($\text{Al}_2(\text{SO}_4)_3 \cdot 18\text{H}_2\text{O}$, Fluka) were used as silica and aluminum sources, respectively. In a typical synthesis, 8g of P123 was added to 60ml of water, and stirred until a clear solution were formed. Different concentrations of HCl (0, 0.1, 0.5, 2, and 5M) were added, and kept stirring for 2 hours. Then 18 g of TEOS and different concentrations of $\text{Al}_2(\text{SO}_4)_3 \cdot 18\text{H}_2\text{O}$ were added respectively, and stirred vigorously at 40°C for 24h. Subsequently, the mixture was transferred to an autoclave and heated at 100°C for 2 days under static condition. The solid precipitate was recovered by filtration, washed several times with distilled water until no Cl^- was detected. The solid product was dried at 60°C overnight, and calcinated at 600°C for 6 hours in air (ramp $2^\circ\text{C}/\text{min}$). The samples prepared from starting gel $\text{SiO}_2/\text{Al}_2\text{O}_3$ molar ratio 20 were designed as Meso-0, Meso-0.1, Meso-0.5, Meso-2, meso-5, the number indicated the HCl concentration added.

2.2. Catalyst Characterization

The sample texture property (surface areas, pore volumes, pore sizes, and pore size distributions) was characterized by using a physisorption analyser of Micromeritics, ASAP 2420 instrument. Before adsorption, the samples were calcined at 823K for 4 hours. 30-40 mg of powder samples were degassed in a sample preparation station under 473K and 1.33×10^{-3} Pa for 15 hours, then switched to the analysis station for adsorption and desorption under liquid nitrogen at 77K with an equilibrium time of 2 minutes. The surface area was calculated with the multipoint BET equation with linear region in the P/P_0 range of 0.05 to 0.35. Pore volume was calculated from the maximum adsorption amount of nitrogen at $P/P_0 = 0.99$. The pore size distribution was determined based on the BJH method and the desorption branch of the isotherm.

The ammonia temperature programmed desorption (NH_3 -TPD) test was conducted with Micromeritics AutoChem 2910 instrument. Prior the TPD measurements, the sample was pre-treated with helium carrier gas at 500°C for 60 min, and cooled down to 50°C . After that, the sample was exposed to 10% NH_3 in He for 30 min followed by purged with helium gas at 100°C for 60 min. to remove the physisorbed ammonia. The TPD run was then conducted from 50 to 700°C at a heating rate of $10^\circ\text{C}/\text{min}$.

Small Angle X-ray Scattering (SAXS) and XRD characterization was performed with the RIGAKU ULTIMA-IV multiple-purposed X-ray diffraction system. SAXS and XRD of the calcinated samples were recorded in the 2θ range from 0.5° to 6° and from 0.5° to 70° respectively using $\text{CuK}\alpha$ radiation ($\lambda = 1.5406$) and proportional counter as detector.

^{29}Si and ^{27}Al MAS NMR were performed on Bruker 400 MHz with spinning rate 4000 Hz. The samples were taken in a zirconium rotor. For ^{29}Si , CP MAS experiment was applied.

For ^{27}Al , one pulse experiment was applied. The chemical shift scales were referenced against ^{29}Si NMR resonance of pure powder silicon at 0 ppm for ^{29}Si NMR, and externally against ^{27}Al NMR resonance of aluminum sulfate at 0 ppm for ^{27}Al NMR.

The pore sizes and wall thickness of the samples were determined by transmission electron microscopy (TEM) on a JEOL 2010 STEM, operated at 200 keV. A small amount of powder (0.5-1.0 g) was mixed with methanol and agitated for 1 minute, and then sonicated for 20 minutes. Several drops of the suspension were placed onto a carbon-coated 3.5mm diameter copper mesh grid before TEM characterization.

The silica and alumina content in the samples was analyzed by using VARIAN VISTA PRO ICP-OES (Inductively Coupled Plasma- Optical Emission Spectroscopy) based on ASTM D1976.

3. Results and Discussion

The isotherms of all product samples from nitrogen adsorption analysis showed the typical type-IV curves. The hysteresis loops indicate the presence of the mesopores. For the samples with initial $\text{SiO}_2/\text{Al}_2\text{O}_3$ molar ratio 20, the effect of acid concentration on relative surface area, pore volume, average pore size, and pore size distribution is illustrated in Figure 1 to Figure 4 respectively. The surface area reaches the maximum at 0.5M HCl and then quickly dropped. The pore volume and average pore sizes exhibit a different trend. They dramatically decreased with increased acid concentration from acid free to 0.1M HCl, then changes become slow or level off while HCl acid concentration changed from 0.5 to 5.0M. With the HCl acid concentration increased, the pore size distribution shifted to smaller pore sizes, and distribution become much wider.

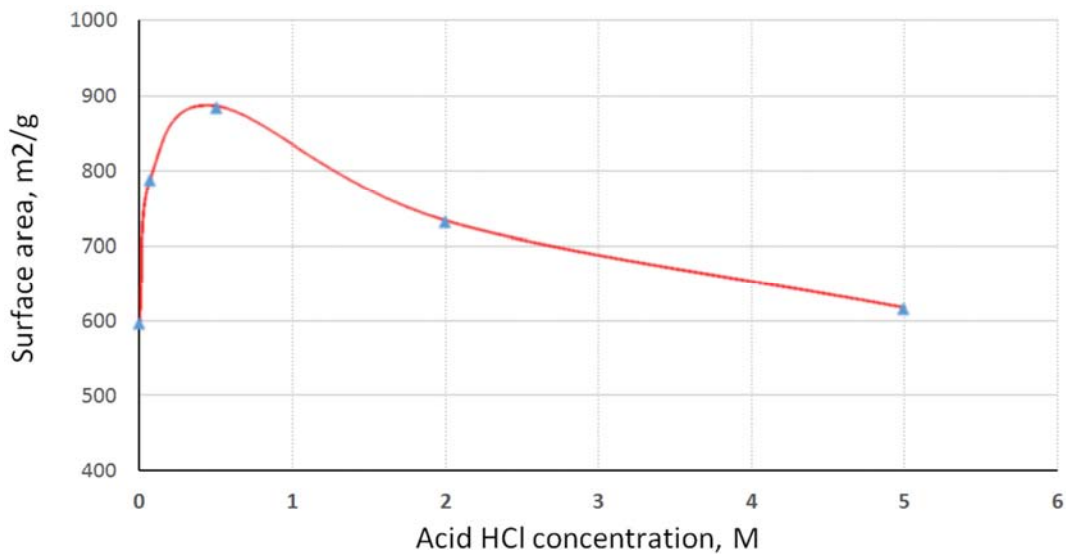


Figure 1. Effect of HCl acid concentration on surface area of the samples.

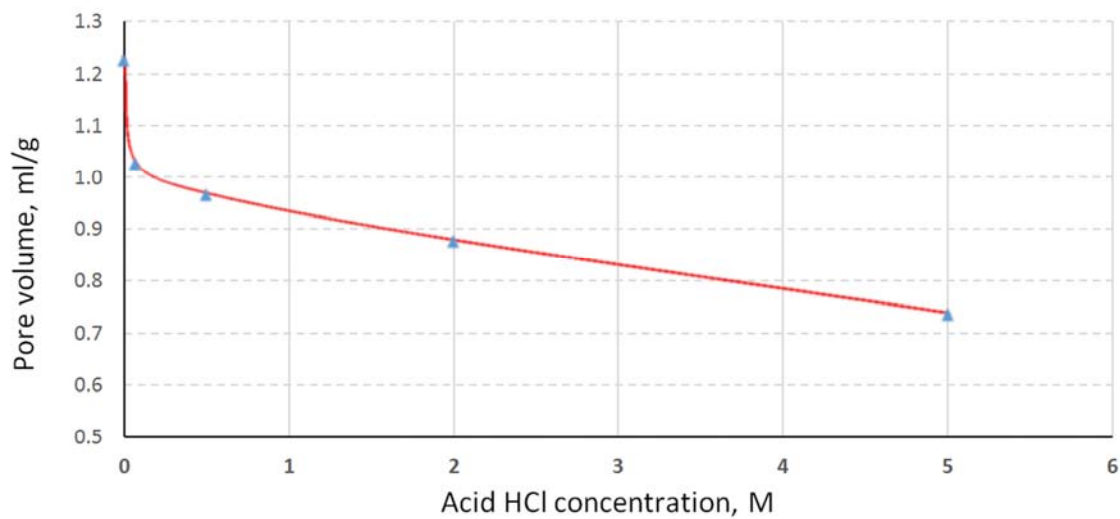


Figure 2. Effect of acid concentration on pore volume of the samples.

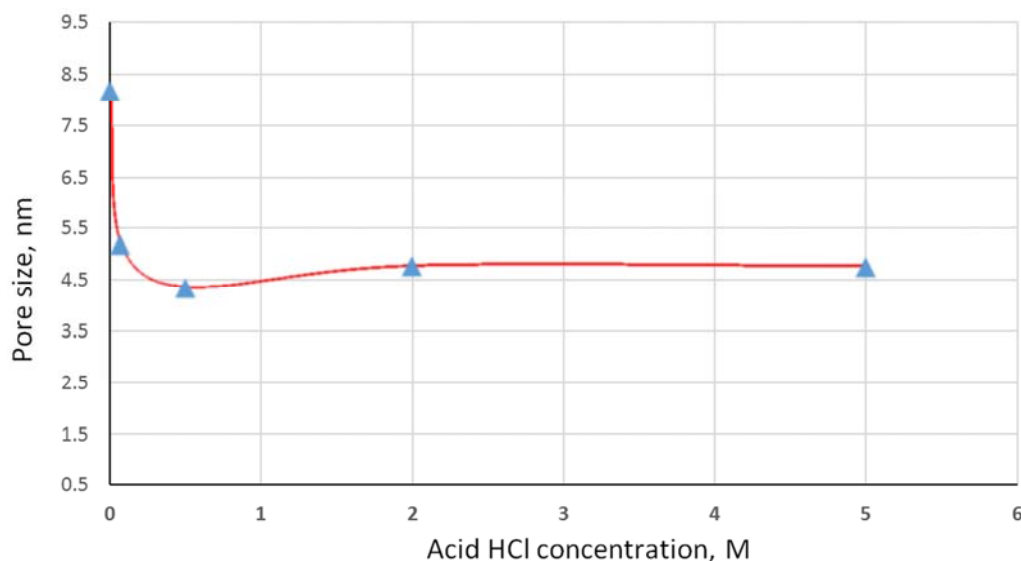


Figure 3. Effect of acid concentration on average pore sizes of the samples.

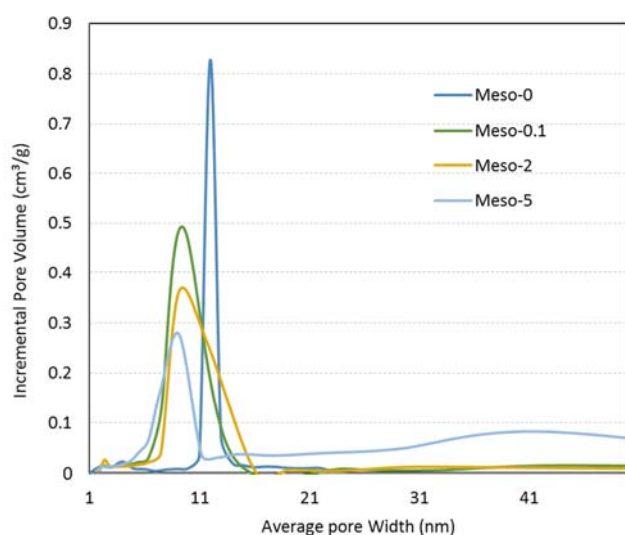


Figure 4. Effect of acid concentration on pore sizes and distributions.

The effect of the $\text{SiO}_2/\text{Al}_2\text{O}_3$ ratio in the initial gels on the textual properties is summarized in Table 1. Under the same HCl acid concentrations, the relative surface areas, pore volumes, and average pore sizes were quite similar. This

means that the initial $\text{SiO}_2/\text{Al}_2\text{O}_3$ ratio did not lead to significant textual property change.

Table 1. Effect of the $\text{SiO}_2/\text{Al}_2\text{O}_3$ ratio in the initial gels on textual properties.

HCl concentration, M	Acid free			0.5		
Initial Si/Al gel molar ratio	5	20	50	5	20	50
Relative surface area, m^2/g	575	600	544	879	887	920
Pore volume, ml/g	1.20	1.23	1.24	1.04	0.97	0.98
Average pore size, nm	8.4	8.2	8.8	5.3	5.0	5.4

The higher surface areas of the catalysts can provide more active sites. The larger pore volume and pore sizes favor the large molecules diffusion and mass transfer, and thus favor the hydroconversion of the heavier petroleum feedstocks. Therefore, from the textual property point of view, the optimized acid concentration of the mesoporous materials synthesized is very low acid environment (acid free or $<0.1\text{M}$).

The acidities and their distribution of Meso-0 to Meso-5 are summarized in Table 2 and illustrated in Figure 5. To compare the acidity distribution among the samples, the weak, medium, and strong acidities were assigned to the peak areas of NH_3 -TPD curves below 623 K, at 623–773 K, and above 773 K, respectively.

Table 2. NH_3 -TPD acidity of the samples.

	Meso-0	Meso-0.1	Meso-0.5	Meso-2	Meso-5
Total acidity, mmol/g	0.36	2.77	0.09	0.08	0.08
Weak acid	0.12	1.24	0.03	0.03	0.03
Medium acid	0.03	0.33	0.01	0.01	0.01
Strong acid	0.20	1.20	0.05	0.04	0.04
Peak temperature, $^\circ\text{C}$					
T1	205	215	200	180	150
T2	555	560	550	550	540

Meso-0.1 exhibited the highest acidity, about 7.7 times higher than that of Meso-0 and about 35 times higher than that of Meso-0.5 to Meso-5. Total acidity and acid distribution became the same when the HCl concentration was $>0.5\text{M}$. With the HCl concentrations increased from

acid-free to 5.0M , the weak acidic peak temperature was shifted to lower temperature, while the strong acid peaks were similar. From acidity distribution, it can be concluded that the majority acidity is weak and strong acidic sites. The weak acidic sites were mainly contributed by alumina and

amorphous silica-alumina, while the strong acidic sites were from tetra-hedral aluminum species. XRD diffraction showed typical amorphous profiles for all samples, indicating not ordered structure in the long range (the XRD spectra are not shown in the communication). The ^{27}Al NMR provided the evidence of the tetra-hedral aluminum species existence. From the effect of the initial $\text{SiO}_2/\text{Al}_2\text{O}_3$ molar ratio in starting gel on the $\text{SiO}_2/\text{Al}_2\text{O}_3$ molar ratio of the final products (Table 3), it can be seen that the final product $\text{SiO}_2/\text{Al}_2\text{O}_3$ ratio seemed independent on the initial gel $\text{SiO}_2/\text{Al}_2\text{O}_3$ ratio.

The final product $\text{SiO}_2/\text{Al}_2\text{O}_3$ molar ratio was higher than

55. The higher the HCl concentration was, the higher $\text{SiO}_2/\text{Al}_2\text{O}_3$ molar ratio the final products had. This means that Al is more difficult to be assembled to become the wall of the mesoporous material than Si. The acid concentration governed the Al amount that can be combined with silica precursors to become the micelles, and finally assembled around the structure direct agents to form mesoporous materials. At higher HCl concentration, the aluminum is more easily existed in the form of Al^{3+} , and presented in the solution not in the micelles. Interestingly, the lowest final product $\text{SiO}_2/\text{Al}_2\text{O}_3$ molar ratio was achieved when the HCl concentration was at 0.1M not acid-free environment.

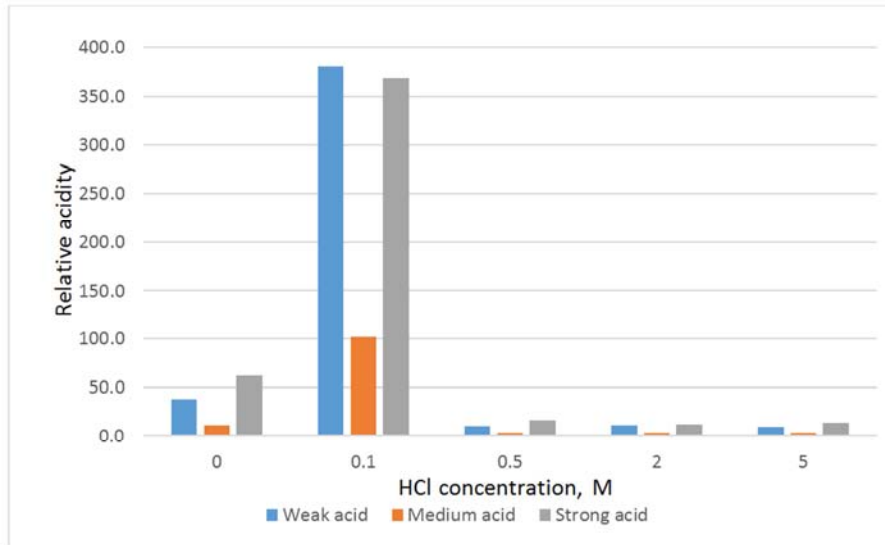


Figure 5. Relative acidity of the sample at different HCl concentration.

Table 3 lists the $\text{SiO}_2/\text{Al}_2\text{O}_3$ molar ratio of the final products under different $\text{SiO}_2/\text{Al}_2\text{O}_3$ molar ratio in starting gel. Although the initial $\text{SiO}_2/\text{Al}_2\text{O}_3$ molar ratio in starting gel increased 10 times (from 5 to 50), the $\text{SiO}_2/\text{Al}_2\text{O}_3$ molar ratio of the final products changed less than 30%. This means that much less Al was assembled in the final mesoporous sample than Si. As expected, when the HCl concentration increase from 0.1M to 5.0M, $\text{SiO}_2/\text{Al}_2\text{O}_3$ molar ratio of the final product abruptly increased.

Table 3. Effect of the initial $\text{SiO}_2/\text{Al}_2\text{O}_3$ molar ratio in starting gel on the $\text{SiO}_2/\text{Al}_2\text{O}_3$ molar ratio of the final products.

$\text{SiO}_2/\text{Al}_2\text{O}_3$ molar ratio in starting gel	5	20	50
$\text{SiO}_2/\text{Al}_2\text{O}_3$ molar ratio in final solid products			
Acid free	58.7	66.6	74
Medium acid (0.1M)	55.4	62.5	72.1
medium acid (0.5M)	267	298	332
Strong acid (2.0M)	-	1061	-
Strong acid (5.0M)	-	1591	-

The comprehensive TEM images of the samples are shown in Figure 6. In the image, the dark and bright strips are the walls and pores of the amorphous materials. About 10-15 such images were selected. The wall thickness and pore sizes were measured. The average wall thicknesses and average pore sizes are illustrated in Figure 7.

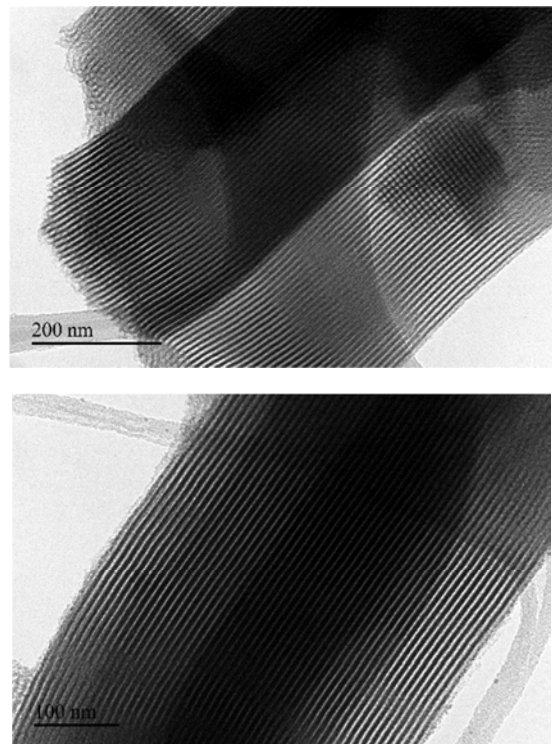


Figure 6. Typical TEM images of the samples.

The wall thickness is dramatically decreased with the HCl concentration, and then level off when HCl concentration was higher than 0.5M. The trend was in good agreement with the BET result. The result was also in agreement with a study on SBA-15 silica synthesized by direct addition of PVA powder [15]. The mesoporous materials with highly ordered structure and thick wall generally showed the excellent thermal and hydrothermal stability. Therefore, from the wall thickness point of view (e.t. thermal and hydrothermal stability), Meso-0 and Meso-0.1 is better than all other samples.

To further prove the formation of the mesopores and the wall thickness, the SAXS characterization was performed and

the results are shown in Figure 8. As seen in Figure 8, all Al-SBA-15 samples exhibit at least two well-resolved peaks indexed to the (100) and (200) reflections which are associated with $p6mm$ hexagonal symmetry. This indicated the samples were of well-ordered meso-structures. With the HCl concentration increased from 0M to 5.0M, the reflection peak (100) was slightly shifted to higher angle, suggesting the unit-cell size of the final sample was decreased. The decreased unit-cell size was one of the reasons that the wall thickness of the samples became thinner when HCl concentration increased.

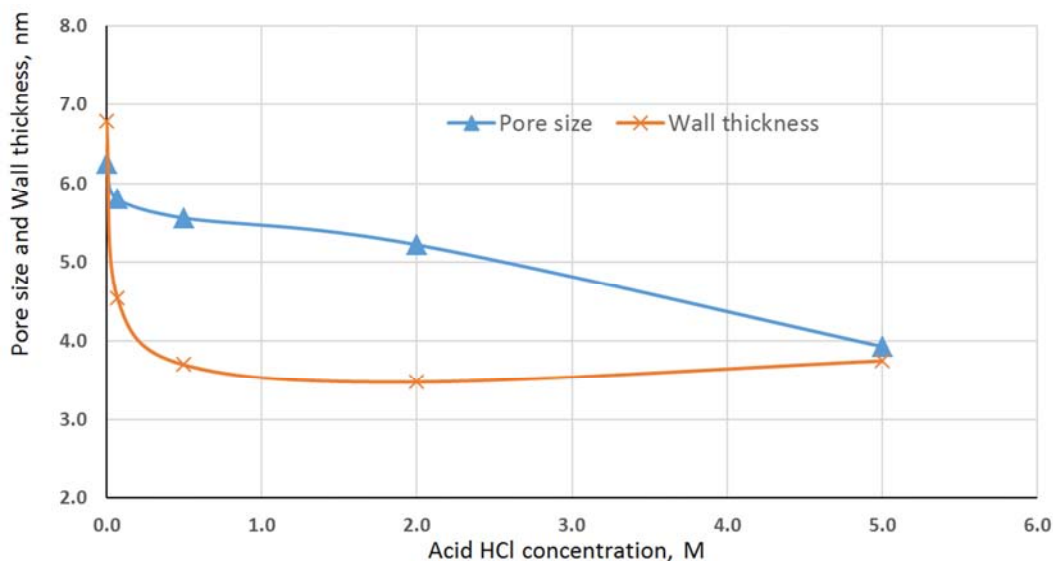


Figure 7. Effect of acid on pore size and wall thickness based on TEM.

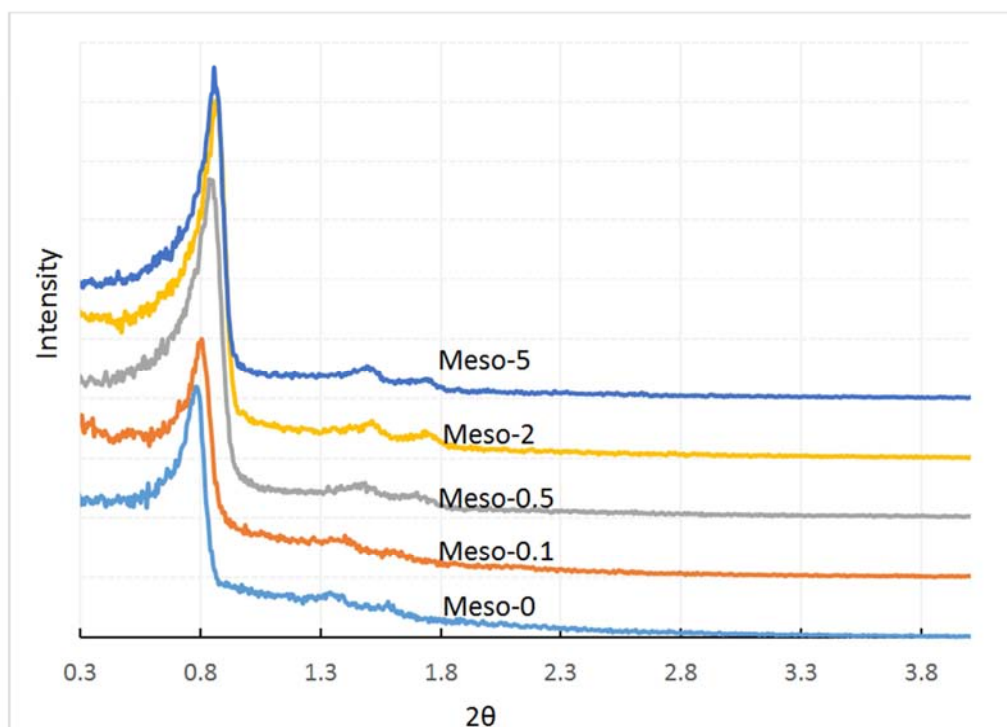


Figure 8. SAXS profiles for the five samples.

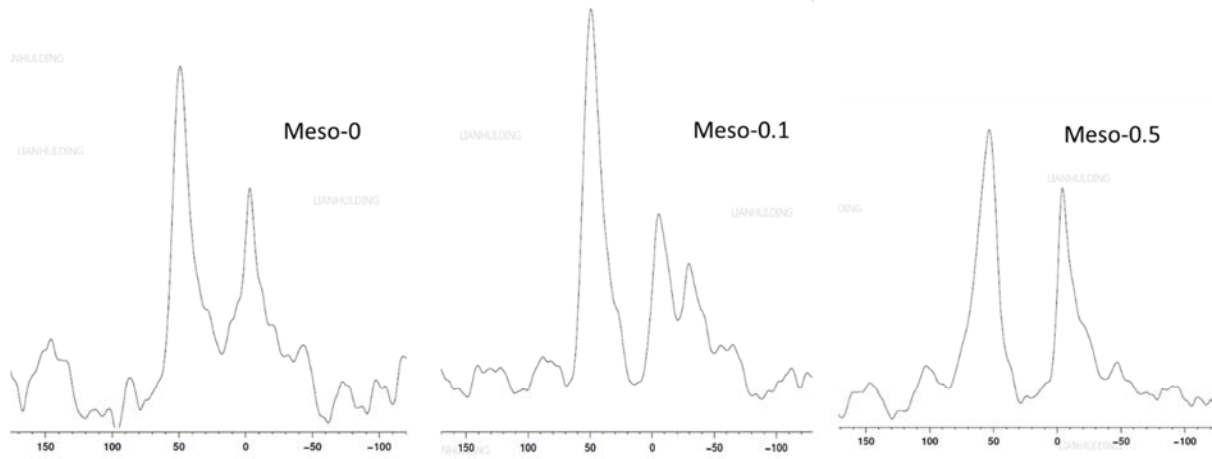


Figure 9. ^{27}Al NMR of Meso-0, Meso-0.1, and Meso-0.5.

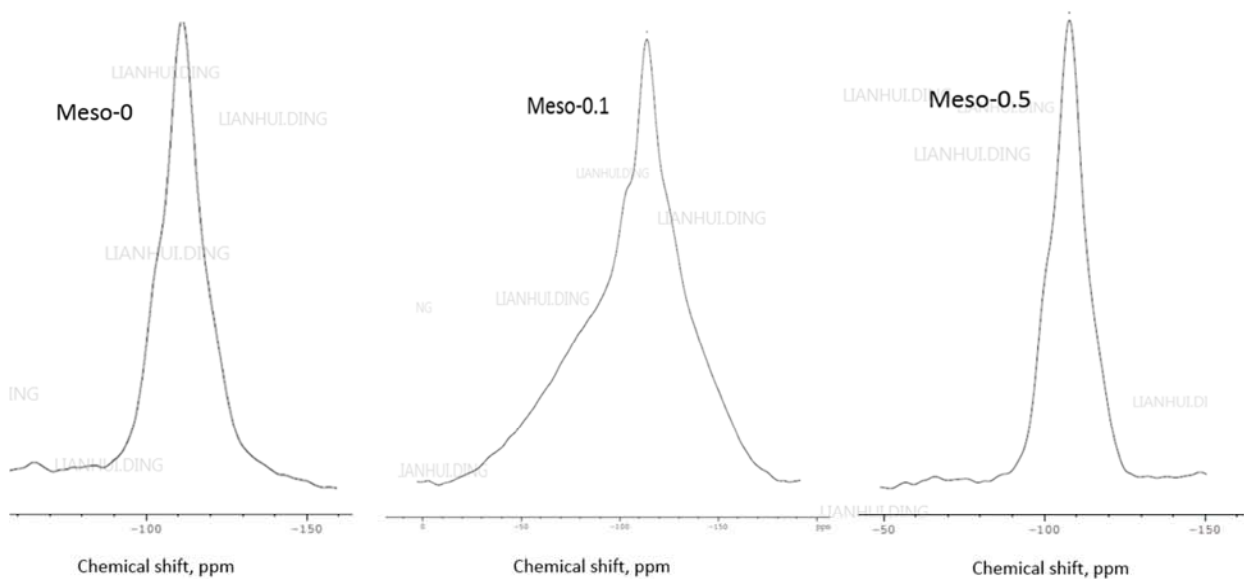


Figure 10. ^{29}Si NMR of Meso-0, Meso-0.1, and Meso-0.5.

^{27}Al MAS NMR spectra of all samples are exhibited in Figure 9. In addition to the band corresponding to tetrahedral Al (the chemical shift: around 40-55 ppm), there was always a band near 0 ppm for all samples, which is attributed to octahedral Al. Appearance of a band in the 25–30 ppm region indicated the presence of penta-coordinated Al [20]. The presence of the tetrahedral Al in all samples explained the existence of the strong acid sites.

The ^{29}Si MAS NMR spectra of Meso-0, Meso-0.1, and Meso-0.5 are illustrated in Figure 10. The resonances around -115 ppm to -109 ppm, -104 ppm, and -96 ppm are assigned to Si(0Al), Si(1Al), and Si(2Al) sites, respectively [19]. No other resonances were identified, indicating the absence of the Si(3Al) and Si(4Al) sites. Meso-0 and Meso-0.5 included only Si(0Al), while there are small quantity of Si(1Al) and Si(2Al) expect for the Si(0Al) for Meso-0.1.

The results from NH_3 -TPD, final product $\text{SiO}_2/\text{Al}_2\text{O}_3$ molar ratio, and ^{27}Al NMR indicate that the highest acidity of Meso-0.1 is closely associated with its high Al content and most of Al species are in the tetrahedral state. Both Lewis and

Bronsted acid sites of the samples are related to the aluminum content in the final product samples and their states (tetrahedral or octahedral coordinated). In the absence of acid and very weak acid environment, the pH value of the P123 solution was about 7, and dropped to about 2-3.5 after dissolution of aluminum sulfate respectively, for initial gel $\text{SiO}_2/\text{Al}_2\text{O}_3$ between 5 and 50. The self-generated acidity from the hydrolysis of aluminum sulfate with the reasonable hydrolysis time was probably effective for the hydrolysis of TEOS. The pH is higher than the isoelectric point of silica (pH=2), and thus positively charged aluminum species is easily interacted with the negatively charged silica species resulting from TEOS hydrolysis. Therefore the aluminum was easily introduced. The initially formed aluminosilicate species possibly are attached to the micelles or even the aluminum cationic species to the micelles facilitating the interaction between micelles and anionic silicate species. This could contribute to the cooperative self-assembly of the organic-inorganic aggregates to form an aluminum rich silicate layer attached to the micelles. At higher acidic

medium (HCl concentration >0.5M), Al species exist only in the cationic form [18]. Due to lower than the isoelectric point of silica, the silica species are also positively charged. Therefore the interaction between Al and Si species in the system was restricted, which makes their condensation with the silica species to form Si-O-Al linkages unlikely. As a result, less Al can be incorporated and assembled with silica micelles, and thus a very high SiO₂/Al₂O₃ molar ratio and lower acidity of the final products were achieved. Other researchers also found that, despite the increase in pH value to 1.5, only a limited amount of Al from the initial gel was incorporated into the final solid products [19-20].

Current study and previous literature proved that weak acidic and acid-free medium favor the synthesis of the Al-SBA-15 with higher acidity and hydrothermal stability that can be applied to hydrocracking and FCC catalysts. Unfortunately, the high Al content in the final product under such condition is hard to be achieved. To synthesize Al-SBA-15 with high content of Al (preferred in tetrahedral form), many methods have been investigated. Li, Jiang and his co-workers used "The hydrolysis-controlled approach" in which the hydrolysis of TEOS was accelerated by fluoride [21-22]. They also tried tetramethylorthosilicate as silicon source instead of TEOS. Lin and his workers used "acid-free approach" (the same as the method in this communication) in which the acidity of the synthesis solution was generated in-situ by the hydrolysis of aluminium sulfate [23]. The disadvantage of all these methods are always still low incorporation of aluminium from the synthesis gel in the final solid and the presence of extra-framework Al species. Therefore, to synthesize mesoporous materials with zeolite structured wall, more studies on proper synthesis conditions, appropriate chemicals, and the order to add them need be carried out to not only ensure the hydrolysis of TEOS, but also the enough interaction between Al and Si species in the synthesis system.

4. Conclusion

When using TEOS and aluminum sulfate as silica and aluminum source respectively, P123 as structure directing agent, the acid free and weak acid environment favored the enhancement of acidity, the formation of larger mesoporous (higher pore volume, pore size, and surface areas), and formation of thicker wall. A considerable amount of Al was in tetrahedral Al state, which help the further conversion to the zeolite wall. The effect of the original gel Si/Al ratio on textural properties and acidity is not significant. The Si/Al molar ratios are all above 50 when the initial Si/Al ratios changed from 5 to 50.

References

- [1] A. Corma, A. Martinez, V. Martinez-Soria, J. B. Monton, *J. of Catal.* 153 (1995) 25-31.

- [2] R. Huirache-Acuna, R. Nava, C. L. Peza-Ledesma, J. Lara-Romero, G. Alonso-Ninez, B. Pawele, E. M. Rivera-Munoz, *Materials* (2013) 4139-4167.
- [3] A. M. Alsobaai, R. Zakaria, B. H. Hameed, *Fuel Processing Technology* 88 (2007) 921-928.
- [4] K. Kohli, R. Prajapati, M. Sau, S. K. Maity, *Procedia Earth and Planetary Science* 11 (2015) 325-331.
- [5] C. T. Kresge, M. E. leonowicz, W. J. Roth, J. C. Vartuli, J. S. Beck, *Nature* 359 (1992) 710.
- [6] A. Corma, *Chem. Rev.* 97 (1997) 2373.
- [7] D. Zhao, Q. Huo, J. Feng, B. F. Chmelka, G. D. Stucky, *J. Am. Chem. Soc.* 120 (1998)6024Al introduce into SBA-15.
- [8] W. Hua, Y. Yue, Zi, Gao, J. *Molecular Catalysis A: Chemical* 170 (2001) 195-202.
- [9] C. Han, H. Wang, L. Zhang, R. Li, Y. Zhang, Y. Luo, X. Zheng, *Advanced Powder Technology* 22(2011)20-25.
- [10] A. A. Campos, L. Martins, L. L. Oliverira, C. R. Silva, M. Wallau, E. A. Urquieta-Gonzalez, *Catalysis Today* 107-108(2005) 759-767.
- [11] H. Kao, C. Ting, S. Chao, *J. of Molecular Catalysis A: chemical* 235 (2005) 200-208.
- [12] K. K. Cheralathan, T. Hayashi, M. Ogura, *Microporous and Mesoporous Materials*, 116 (2008) 406-415.
- [13] M. Baca, E. de la Rochefoucauld, E. Ambroise, J. M. Krafit, R. Hajjar, P. P. Man, X. Carrier, J. Blanchard, *Microporous and Mesoporous Materials* 110 (2008) 232-241.
- [14] J. Wang, H. Ge, W. Bao, *Materials letters* 145 (2015) 312-315.
- [15] S. Lin, L. Shi, T. Yu, X. Li, X. Yi, A. Zheng, *Microporous Mesoporous Material* 207 (2015) 111-119.
- [16] S. Lin, L. Shi, M. M. L. Ribeiro Carrott P. J. M. Carrott, J. Rocha, M. R. Li, X. D. Zou, *Microporous Mesoporous Material* 142(2011) 526-534.
- [17] L. Shi, Y. Xu, N. Zhang, S. Lin, X. Li, P. Guo, X. Li, *Journal of Solid State Chemistry* 203 (2013) 281-290.
- [18] C. Marquez-Alvarez, N. Zikova, J. Perez-Pariente, J. Cejka, *Catal. Rev.* 50(2008) 222.
- [19] Y. Yue, A. Gefeon, J. L. Bonardet, N. Melosh, J. B. D'Espinoze, J. Fraissard, *Chem. Commun.* (1999) 1967-1968.
- [20] B. Dragoi, E. Dumitriu, C. Guimon, A. Auroux, *Micropor. Mesopor. Mater.* 121(2009) 7-17).
- [21] Y. Li, W. Zhang, L. Zhang, Q. Yang, Z. Wei, Z. Feng, C. Li, *J. Phys. Chem. B* 108 (2004) 9739-9744.
- [22] T. Jiang, H. Tao, J. Ren, X. Liu, Y. Wang, G. Lu, *Micropor. Mesopor. Mater.* 142 (2011) 341-346.
- [23] S. Lin, L. Shi, M. M. L. Ribeiro, Carrott, P. J. M. Carrott, J. Rocha, M. R. Li, X. D. Zou, *Micro. Meso. Mater.* 142 (2011) 526-534.